ELSEVIER

applied surface science

Study of the topmost surface structure of a *y*-cut LiNbO₃ single crystal with coaxial impact collision ion scattering spectroscopy (CAICISS)

Takashi Yamada[a], Tetsuo Choso[a,1], Kenji Tabata[a,b,*], Eiji Suzuki[a,b]

[a]*Research Institute of Innovative Technology for the Earth (RITE), 9-2 Kizugawadai, Kizu-cho, Soraku-gun, Kyoto 619-0292, Japan*
[b]*Graduate School of Materials Science, Nara Institute of Science and Technology (NAIST), Takayama-cho, Ikoma-shi, Nara 630-0101, Japan*

Abstract

The topmost surface structures of a *y*-cut LiNbO₃ single crystal were studied with coaxial impact collision ion scattering spectroscopy (CAICISS). The observed CAICISS spectra of the azimuthal intensity variation of Nb atoms of that had mirror plane symmetry which was unexpected from the space group of LiNbO₃ ($R3c$, C_{3v}^6) itself. By the simulation of CAICISS, it was strongly suggested that Nb atoms at the topmost few layers of *y*-cut LiNbO₃ single crystal were rearranged to give a mirror plane of symmetry in their three-dimensional atomic configuration rather than to form other related oxides. © 2001 Elsevier Science B.V. All rights reserved.

1. Introduction

Coaxial impact collision ion scattering spectroscopy (CAICISS) which has been developed from conventional low energy ion scattering spectroscopy (LEIS) is one of the superior method to characterize the topmost surface structure of solids [1,2]. The advantages of CAICISS are related to its apparatus arrangements, in which the detector and the ion source were set coaxially to the sample. These arrangements make the contribution of multiple scattering minimum and possible to get both qualitative and quantitative information on surface structures down to about 10 Å in depth. The usefulness of CAICISS has already been proven. For example, Aono et al. used CAICISS for the in situ observation of film growth in the MBE process [3,4]. In the last 10 years, owing to the development of computer technology, we have been able to perform accurate analysis of surface structure by simulating CAICISS spectra for surface atomic configuration models. Ishiyama et al. identified the topmost structure of SrTiO₃ (0 0 1) by CAICISS with the simulation of azimuthal dependence [5]. Fuse et al. simulated the time of flight (TOF) spectra and incident angle-scan spectra of Sr atoms for TiO₂-terminated SrTiO₃ (0 0 1) [6]. Several simulation programs have

---

* Corresponding author. Tel.: +81-774-75-2305; fax: +81-774-75-2318.
E-mail address: kenjt@rite.or.jp (K. Tabata).
¹ Present address: Technology Research Laboratory, Shimadzu Corporation, Nishinokyo Kuwahara-cho, Nakagyo-ku, Kyoto 604-8511, Japan.

been compared and discussed about their accuracy [5–9].

LiNbO$_3$ is known as a material having piezoelectric and electro-optic properties [10,11], and its reduced surface characters have been studied intensively for their practical importance as electric devices with ultraviolet photoelectron spectroscopy (UPS), Auger electron spectroscopy (AES), electron-energy-loss spectroscopy (EELS) and X-ray photoelectron spectroscopy (XPS) [12–16]. Previously, we studied the topmost surface of a *z*-cut (0 0 1) LiNbO$_3$ single crystal with CAICISS and XPS [17–20]. The CAICISS spectra for the *z*-cut sample as-supplied showed a three-fold symmetry and were in good agreement with the simulation results for the O terminated model [18]. On the other hand, for the *y*-cut LiNbO$_3$ single crystal, it has been reported that Ar-ion or electron beam treatment gives rise to the release of Li and O atoms from the surface, then the formation of reduced niobium ions and the change in the surface chemical composition takes place [12–14]. However, the structural change in the topmost layers of a *y*-cut LiNbO$_3$ is still unclear.

In the present study, we report the results of CAICISS analysis for the topmost surface structures of *y*-cut LiNbO$_3$ single crystal as-supplied and after heat treatment at 400°C in a vacuum chamber. Utilizing the software based on two-atom triple scattering model [7], we simulated CAICISS spectra and compared them with measured ones.

2. Experimental

The single crystal of a *y*-cut LiNbO$_3$ was obtained from Alpha Scientific Co., Ltd. This sample plate was produced by the Czochralski process and mechanically polished to optical finish without any chemical treatment. The size was $13 \times 13 \, mm^2$ and 1 mm in thickness. The sample was a nominal '*y*-cut'. The phase of this sample was identified as a (3 0 0) single crystal of LiNbO$_3$ by X-ray diffraction using monochromatic Cu Kα radiation (Fig. 1). The sample plate was rinsed at room temperature in methanol for 1 h with a ultrasonic cleaner and dried at 40°C in a dry box before each experiment.

The measurements of CAICISS was carried out with CAICISS-I (Shimadzu Corporation) in an ultra
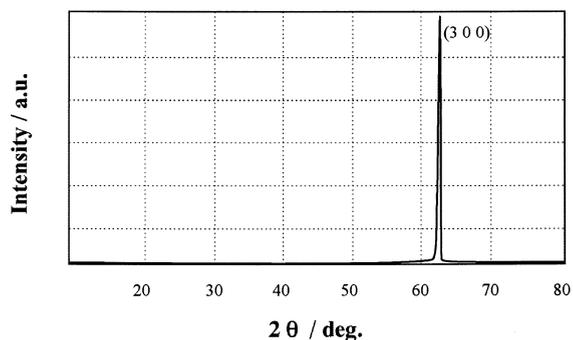
Fig. 1. XRD pattern of as-supplied *y*-cut LiNbO$_3$ single crystal.

high vacuum chamber at 1×10^{-7} Pa. In measurements, the sample was set coaxially to the 3 keV He$^+$ ion source to detect scattered ions at a backscattering angle of 180°. Sample heating was performed indirectly in analysis chamber by a resistivity heater mounted in sample holder which was made of copper. The temperature of the sample was monitored with a themocouple mounted at the distance of 1 mm apart from the top of the sample holder. The estimated measurements error should be within ±10°C. We used two types of software CAMEPRO and COSCAT (Shimadzu Corporation). CAMEPRO was used for the measurements of intensity variations with CAICISS apparatus. The simulation of CAICISS spectrum was carried out by COSCAT. This calculation was based on the two-atom triple scattering model for impact collision ion scattering taking into account the effects of thermal oscillation of atoms [7].

3. Results and discussion

3.1. CAICISS spectra for y-cut LiNbO$_3$ single crystal

Fig. 2 shows the CAICISS spectra for as-supplied (a) and 400°C annealed (b) *y*-cut LiNbO$_3$ single crystal, respectively. These spectra show azimuthal dependence of Nb signal intensity measured at an incident angle of 30°. The peaks of O and Li atoms in the TOF spectra were not discernible because of their low S/N ratio. The incident angle was measured from the normal line to the sample. The peaks in the TOF spectra consist of the contributions of atoms from the topmost surface down to a few tens layers in the depth.
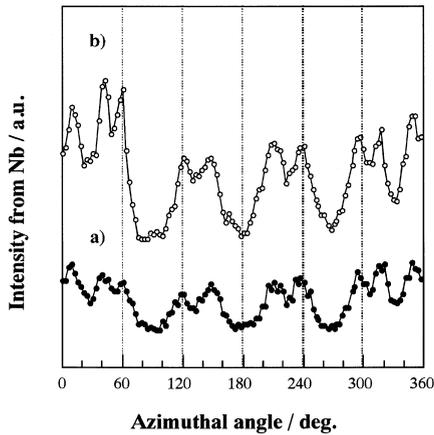
Fig. 2. Azimuthal dependence of Nb signal intensity at incident angle of $30°$. (a) as-supplied; (b) after annealing at $400°C$.

The intensity variations in Fig. 2 reflect the results of shadowing and focusing effects of a shadow cone. Observed spectra, both for the as-supplied and the $400°C$ annealed sample, had peaks at 180 ± 30, ± 60, ± 120, ± 140 and $\pm 170°$. This means that the structure in the topmost layers of $LiNbO_3$ has a mirror plane of symmetry. After $400°C$ annealing in a vacuum chamber, the symmetry of the spectrum became clearer. It might be because of the rearrangements in the topmost layers and the removal of surface contaminants.

Previously, Courths et al. [12,13] investigated the surface properties of Ar-ion or electron-beam bombarded *y*-cut $LiNbO_3$ single crystal at room temperature with UPS and XPS, and reported that the $LiNbO_3$ crystal lost Li_2O by these treatments and the surface was reduced until the chemical compositional formula reached to $LiNb_3O_8$. They reported that oxygen vacancies were formed by the release of Li_2O, and furthermore, Nb^{4+}, Nb^{3+} and unknown negatively charged defects were formed. Cháb and Kubátová [14], however, claimed another explanation of the effects for the electron-beam heating. According to them, electron-beam heating removed the surface vacancies of oxygen and lithium by ordering the surface into $LiNbO_3$ and Nb_2O_5 regions without considering the diffusion of ions from the bulk of $LiNbO_3$. It could be expected that such reorganization was possible only in the outermost layers of the surface. On the other hand, the phase diagram of Li_2O-Nb_2O_5 system have indicated the presence of two stable

solids, $LiNb_3O_8$ and $Li_2Nb_{28}O_{71}$, in the range from $LiNbO_3$ to Nb_2O_5 [21]. Therefore, if the sample lost a part of Li and O atoms, and if the topmost surface layers were reorganized and crystallized to form stable single structure such as $LiNb_3O_8$, that should be characterized by CAICISS. Since the crystal structure of $LiNbO_3$, $LiNb_3O_8$ and Nb_2O_5 have been reported, we examined the CAICISS simulations of the azimuthal angle dependence of Nb atoms for them with simulation software, COSCAT.

3.2. CAICISS simulations for $LiNbO_3$, $LiNb_3O_8$ and Nb_2O_5

The ideal arrangement of $LiNbO_3$ crystal and its $(3\ 0\ 0)$ plane are illustrated in Fig. 3. $LiNbO_3$ is a rhombohedral with lattice constants $a = 5.184$ Å and $b = 13.586$ Å [22]. The space group of $LiNbO_3$ ($R3c$, $C_{3v}{}^6$) indicates that no mirror plane of symmetry exists while measured spectra (Fig. 2) had mirror plane symmetry. Fig. 4 provides simulated CAICISS spectra of azimuthal dependency of Nb signal for $LiNbO_3$ $(0\ 0\ 1)$ and $(3\ 0\ 0)$ at an incident angle of $30°$. The azimuthal angle increased counter-clockwise from the start position. The simulated spectrum for $(0\ 0\ 1)$ plane clearly showed three-fold symmetry and was different from the measured one. Thus, the sample surface could be assumed not to be rearranged to form $(0\ 0\ 1)$ plane. On the other hand, the simulated result for $(3\ 0\ 0)$ plane did not possess apparent symmetry, but the peaks at 180 ± 30, ± 80, ± 100, ± 140 and $\pm 160°$ seemed to represent an uncertain mirror plane of symmetry in the $[0\ 1\ 0]$ azimuth.

The simulated CAICISS spectra for some planes of $LiNb_3O_8$ are provided in Fig. 5. We carried out CAICISS simulations for $(1\ 0\ 0)$, $(3\ 0\ 0)$, $(0\ 1\ 0)$ and $(0\ 0\ 1)$ planes because we could not predict finally stabilizing plane of the topmost layer during the reorganization from $LiNbO_3$ to $LiNb_3O_8$. $LiNb_3O_8$ is a monoclinic with lattice constants a, b, c and β of 15.262, 5.033, 7.457 Å and $107.34°$, respectively [23]. The space group of $LiNb_3O_8$, $P2_1/c$, suggested the absence of mirror plane symmetry, however, the spectrum of $(0\ 0\ 1)$ plane gave an uncertain mirror plane of symmetry parallel to *a*-axis (Fig. 5d). This spectrum had peaks mainly at 180 ± 15, ± 30, ± 70, ± 100, $\pm 140°$, respectively. The peak position and intensity variation were not in agreement with the measured
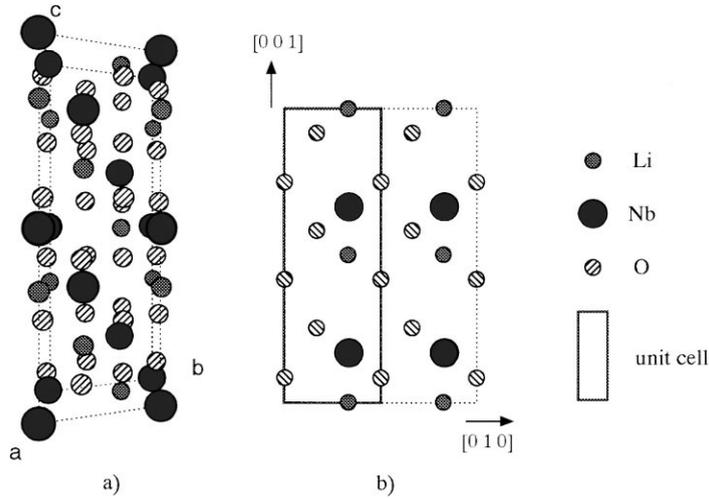
Fig. 3. The ideal structure of $LiNbO_3$ (a) crystal and (b) (3 0 0) plane.

spectra for the *y*-cut sample. The results for the other planes, (1 0 0), (3 0 0) and (0 1 0), gave randomly arranged peaks and did not represent any symmetry.

Nb_2O_5 has been known as a polymorph crystal and its modification of crystal has been well studied [24,25]. Brauer reported that amorphous niobium oxide begins to crystallize to a low temperature (*T*-) form Nb_2O_5 at 500°C [24]. Schäfer et al. reported that the crystallization to *T*-form Nb_2O_5 occurred at 430°C [25]. Since the pre-treatment temperature of the sample was 400°C, the presence of amorphous and/or

T-form Nb_2O_5 was considerable. When amorphous Nb_2O_5 is formed on $LiNbO_3$ surface, intensity variation is never observed in a CAICISS spectrum. Thus
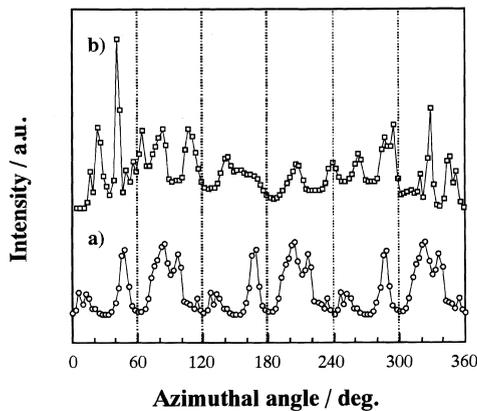
Fig. 4. Simulated CAICISS spectra for $LiNbO_3$ (a) (0 0 1) and (b) (3 0 0) at the incident angle of 30°. Start directions were [0 $\bar{1}$ 0] and [0 1 0], respectively.
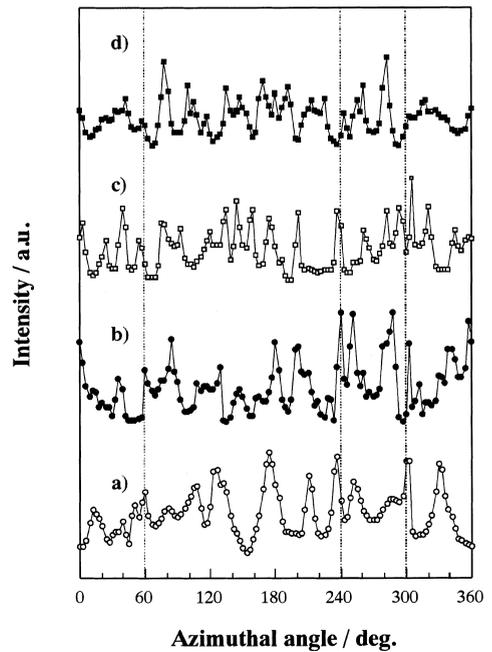
Fig. 5. Simulated CAICISS spectra for $LiNb_3O_8$ (a) (1 0 0), (b) (3 0 0), (c) (0 1 0) and (d) (0 0 1) at incident angle of 30°. Start directions were [0 1 0] for (a) and (b), [0 0 1] and [1 0 0], respectively.

only T-Nb_2O_5 was discussed. T-Nb_2O_5 is a monoclinic crystal and the lattice constants are $a = 6.175$ Å, $b = 29.175$ Å and $c = 3.930$ Å, respectively [26]. The space group of T-Nb_2O_5, *Pbam*, allows to have a mirror plane of symmetry in the planes parallel to (1 0 0) and (0 1 0) and two-fold symmetry in (0 0 1). The simulated results showed the presence of mirror plane of symmetry for (1 0 0), (3 0 0) and (0 1 0) (Fig. 6). The simulated spectrum for (0 0 1) presented two types of symmetry, i.e. a two-fold and a mirror plane symmetries parallel to *a*- and *b*-axis. Many peaks were observed in each spectrum but their positions and intensities were not in accordance with the measured one.

3.3. CAICISS simulations for arranged LiNbO₃ (3 0 0)

As shown in a previous section, the suggested crystals used for CAICISS simulations did not give a satisfied result, then we examined to the structural change of $LiNbO_3$ (3 0 0). Previously, we revealed with temperature programmed desorption that $LiNbO_3$ released Li atoms easily as Li_2O above 400°C [18]. Where the change in the lattice constants and the positions of O and Nb atoms accompanied by the release of Li atoms were not taken into consideration, we prepared model of $LiNbO_3$ (3 0 0) omitting Li atoms from the topmost three layers and used it for the
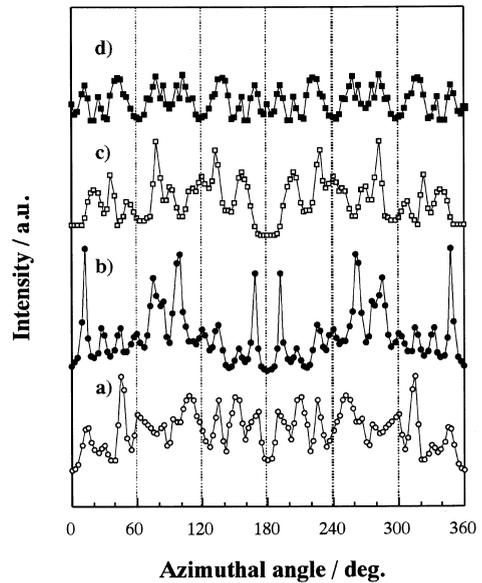
Fig. 6. Simulated CAICISS spectra for T-Nb_2O_5 (a) (1 0 0), (b) (3 0 0), (c) (0 1 0) and (d) (0 0 1) at incident angle of 30°. Start directions were [0 1 0] for (a) and (b), [0 0 1] and [1 0 0], respectively.

simulation. The topmost two layers of those models are shown in Fig. 7.

In the case of Fig. 7a, the loss of Li atoms produced both a two-fold and a mirror plane symmetries in the [0 1 0] azimuthal direction in the model. However, the
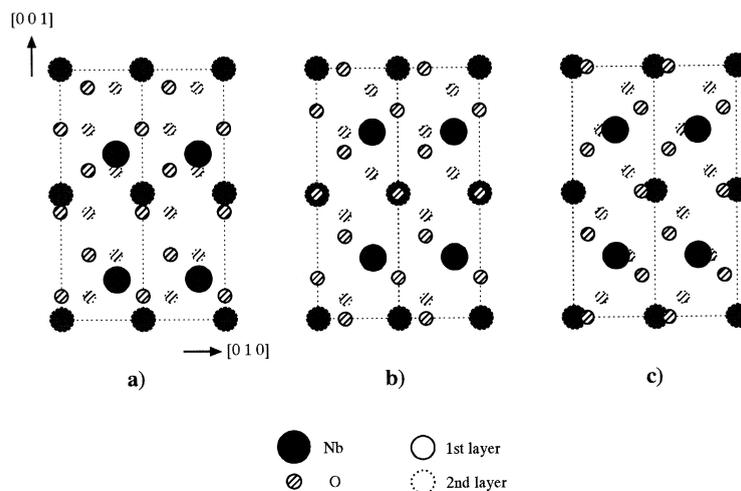
Fig. 7. Topmost two layers of arranged LiNbO₃ (3 0 0). Each configuration represents the model (a) having no Li, (b) whose topmost layers of (a) was displaced for 1.280 Å to [0 0 1] direction, (c) whose topmost layers of (b) was displaced for 1.728 Å to [0 $\bar{1}$ 0] direction.
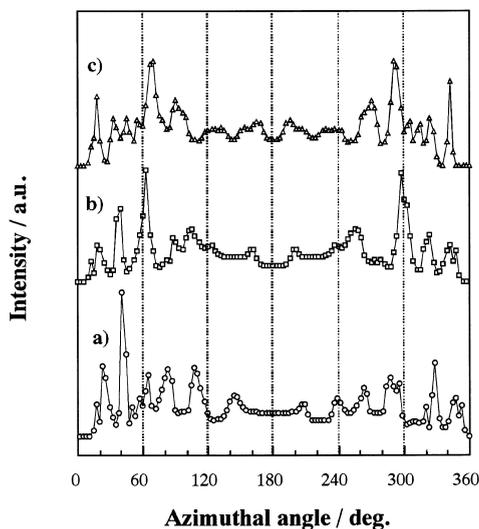
Fig. 8. Simulated CAICISS spectra for the arranged LiNbO$_3$ (3 0 0) for the model of (a), (b) and (c) in Fig. 7, respectively. Start direction is [0 $\bar{1}$ 0] azimuth.

simulated spectrum (Fig. 8a) was changed only in the range of 140–200° from that of the original structure (Fig. 3b) and did not have a two-fold symmetry. Thus, it is clear that Li atoms in LiNbO$_3$ (3 0 0) affect a little to the He$^+$ ion scattering by Nb atoms.

Therefore, we assumed the configuration of Nb atoms is the most important factor, then we made two rearranged models. We considered to give a mirror plane of symmetry to the three-dimensional configuration of Nb atoms with smallest sift from the model of Fig. 7a. The models are shown in Fig. 7b and c. In these models, each layer was slid (b), for 1.282 Å along *b*-axis; (c), for 1.282 and 0.864 Å along *b*- and *c*-axis from the model in Fig. 7a, respectively. The views of rearranged models gave a clear mirror plane symmetry to the three-dimensional configuration of Nb atoms. The symmetry plane of each model was in the direction of [0 1 0] azimuth. The simulated spectra are shown in Fig. 8b and c. The peak positions of these spectra were (b), 180 ± 20, ± 80, ± 115, ± 140 and $\pm 160°$, and (c), 180 ± 20, ± 50, ± 90, ± 110 and $\pm 160°$, respectively. Both spectra possessed obviously a mirror plane of symmetry in the [0 1 0] azimuth as discussed above. O atoms would cause a disagreement from a plane symmetry. Especially, the peak positions in Fig. 8b is fairly good agreement with the measured one, though it still has differences in intensities.

Therefore, it was suggested that the surface layers of (3 0 0) LiNbO$_3$ were rearranged to have a mirror plane of symmetry in the configuration of Nb atoms like Fig. 8b after the release of Li atoms. In actual surface, the rearrangement of O atoms surrounding Nb and the migration of Nb atoms to the perpendicular direction to the (3 0 0) plane should be considered during the rearrangements to achieve the configuration possessing a higher mirror plane of symmetry.

4. Conclusion

The topmost structure of the *y*-cut single crystal of LiNbO$_3$ (3 0 0) was elucidated by means of CAICISS. The measured spectra of azimuthal dependence of Nb signal had a mirror plane of symmetry which was not expected from its crystal structure. The simulated spectra for the rearranged structure models without Li atoms at the topmost few layers gave a mirror plane of symmetry. Therefore, the topmost surface layers lost Li atoms and rearranged to possess a mirror plane symmetry in the configuration of Nb atoms rather than the formation of other suggested related phases such as LiNb$_3$O$_8$ and *T*-form Nb$_2$O$_5$.

References

[1] H. Nichus, W. Heiland, E. Taglauer, Surf. Sci. Rep. 17 (1993) 213.
[2] M. Katayama, E. Nomura, N. Kanekama, H. Soejima, M. Aono, Nucl. Instrum. Methods Phys. Res. B 33 (1988) 857.
[3] M. Katayama, T. Nakayama, C.F. McConville, M. Aono, Nucl. Instrum. Methods Phys. Res. B 99 (1995) 598.
[4] M. Katayama, T. Nakayama, M. Aono, C.F. McConville, Phys. Rev. B 54 (1996) 8600.
[5] O. Ishiyama, T. Nishihara, S. Hayashi, M. Shinohara, M. Yoshimoto, T. Ohnishi, H. Koinuma, S. Nishio, J. Saraie, Appl. Surf. Sci. 121/122 (1997) 163.
[6] T. Fuse, O. Ishiyama, M. Shinohara, Y. Kido, Surf. Sci. 372 (1997) 350.
[7] R.S. Williams, M. Kato, R.S. Daley, M. Aono, Surf. Sci. 225 (1990) 355.

[8] T.C.Q. Noakes, D.A. Hutt, C.F. McConville, D.P. Woodruff, Surf. Sci. 372 (1997) 117.

[9] T. Fuse, M. Watanabe, Y. Kido, O. Ishiyama, M. Shinohara, F. Ohtani, Surf. Sci. 357/358 (1996) 119.

[10] A. Räuber, in: E. Kaldis (Ed.), Current Topic in Materials Science, Vol. 1, Amsterdam, 1978, p. 481.

[11] EMIS Data Review Series No. 5. Properties of Lithium Niobate, Institution of Electrical Engineers, London, 1989.

[12] R. Courths, P. Steiner, H. Höchst, S. Hüfner, Appl. Phys. 21 (1980) 345.

[13] R. Courths, P. Steiner, H. Höchst, S. Hüfner, Ferroelectrics 26 (1980) 745.

[14] V. Cháb, J. Kubátová, Appl. Phys. A 37 (1986) 67.

[15] V.H. Ritz, V.M. Bermudez, Phys. Rev. B 24 (1981) 5559.

[16] O.F. Schirmer, D. von der Linde, Appl. Phys. 33 (1978) 35.

[17] T. Choso, M. Kamada, K. Tabata, Appl. Surf. Sci. 121/122 (1997) 387.

[18] K. Tabata, T. Choso, Y. Nagasawa, Surf. Sci. 408 (1998) 137.

[19] K. Tabata, T. Choso, A. Murakami, E. Suzuki, Surf. Sci. 402–404 (1998) 487.

[20] K. Tabata, T. Choso, Y. Nagasawa, Surf. Sci. 433–435 (1999) 534.

[21] E.M. Levin, H.F. McMurdie, in: M.K. Reser, (Ed.), Phase Diagrams for Ceramists 1975 Supplement, The American Ceramic Society, 1975, p. 86.

[22] S.C. Abrahams, H.J. Levinstein, J.M. Reddy, J. Phys. Chem. Solids 27 (1966) 997.

[23] M. Lundberg, Acta Chem. Scand. 25 (1971) 3337.

[24] G. Brauer, Z. Anorg. Allg. Chem. 248 (1941) 1.

[25] H. Schäfer, R. Gruehn, F. Schulte, Angew. Chem. 78 (1966) 28.

[26] K. Kato, S. Tamura, Acta Cryst. B 31 (1975) 673.